RSC Advances

ROYAL SOCIETY OF CHEMISTRY

www.rsc.org/advances
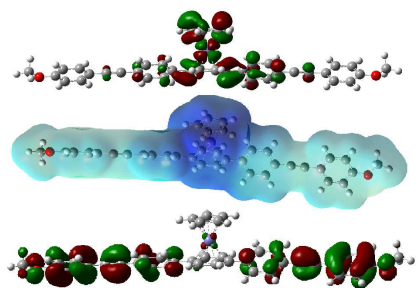
With the enlarged and annulated ICT conjugation systems, three new cationic cyclopentadienyliron complexes with double 4-methoxy diphenylethynyl-substituted arenas synthesized in this paper exhibited significantly better third-order NLO absorption properties than the commercial cyclopentadienyliron arene complexes I-261.

RSC Advances

ARTICLE

Synthesis and Optical Properties of Novel D-π-A-π-D Type Cationic Cyclopentadienyliron Complexes of Arenes †

B. D. Zhao,[b] G. L. Li,[b] Y. Z. Shi,[b] H. Q. Zhang [b] and T. Wang[*a,b]

Diphenylethynyl chromophores were successfully introduced into the arene ligands of cationic cyclopentadienyliron complexes through nucleophilic substitution and Suzuki coupling reactions. Three novel cationic cyclopentadienyliron complexes with symmetrical di(4-methoxy-phenylethynyl) chromophores (CFSs) were obtained and completely characterized by IR, ^{1}H NMR, ^{13}C NMR, and MS. The linear and nonlinear optical properties of the obtained molecules were tuned using phenylethynyl linkages. The UV–vis absorption spectra showed that increasing the conjugation by substituting phenylacetylene spacer resulted in a red shift in the absorption bands and a stronger absorption in CFSs than in the previously reported (η^6-cumene) (η^5-cyclopentadienyl) iron hexafluorophosphate (I-261). These cross-conjugated D-π-A-π-D type compounds also showed larger third-order nonlinear susceptibility than I-261.

Introduction

Conjugated organometallic complexes are considered as potential optical materials because of the coordination centers of their metal complexes, which offer a great diversity in terms of electronic properties.[1] As an important kind of organometallic complexes, ferrocene-based architectures bearing an unsaturated backbone with unique chemical, photochemical, and electrochemical properties play an important role in the design of functional materials.[2]

Materials exhibiting large two-photon absorption (TPA) are currently of great interest because of their applications in various fields such as multiphoton fluorescence microscopy, three-dimensional (3D) optical data storage, optical power limiting, and microfabrication.[3] To fully exploit the great potential of the TPA process, search for new compound exhibiting large δ values is still one of the hot topics in the field of functional materials. General design strategies are to develop molecules with large changes of dipole/quadrupole moments upon excitation, with extended conjugation, etc.[4] This can be achieved through structure motifs such as D-π-A, D-π-D, D-π-A-π-D, and A-π-D-π-A.[5] Among these molecules, the D-π-A-π-D structure is highlighted by its excellent TPA property, and the presence of A as the core induces charge transfer from the periphery to the center of the molecule which hence enables the molecule to display a large two-photon absorption cross-section.[6]

Besides organic TPA molecules, organometallic/coordination compounds have received considerable interests for the third-order nonlinear optical (NLO) applications, and some complexes, such as Nickel, Iron, Zinc, Ruthenium complexes and so on, have been reported to exhibit interesting TPA properties, showing remarkable progress.[7] Cationic cyclopentadienyl iron complexes (Fc-arene) is different from ferrocene. These complexes have different arene ligands and exhibit diverse spectral characteristics and functionality. Unlike ferrocene, Fc-arene is a good electron acceptor and is susceptible to attack by nuleophiles.[8] However, to the best of our knowledge, a study on Fc-arene with TPA properties has not been reported, and a study on Fc-arene with a diphenylacetylene-linkaged backbone has also not been reported.

Fc-arene is an important kind of cationic photoinitiators. Mechanism of the photoinitiation of Fc-arenes is that Fc-arenes undergo photolysis to generate an iron-based Lewis acid upon the loss of the arene ligand. Coordination of this latter species with an epoxy monomer is followed by ring-opening polymerization. The ring-opening and the polymerization reaction start in the ligand sphere of the iron (II) cation due to its lack of electrons. As photoinitiators, these complexes are attractive because they have different arene ligands and exhibit diverse spectral characteristics and functionality.[9] Two-photon polymerization (TPP) has attracted much attention in recent years as a powerful tool for realizing high-density optical data storage and three-dimensional microfabrication of functional devices.[10] To improve the performance of TPP, initiators with large two-photon absorption (TPA) cross sections and high initiating efficiencies are required.

Three cationic cyclopentadienyliron complexes of arenes with D-π-A-π-D structures were synthesized via nucleophilic

[a.] State Key Laboratory of Chemical Resource Engineering, College of Science, Beijing University of Chemical Technology, Beijing 100029, PR China. E-mail: wangtwj2000@163.com. Tel.: 0086-010-64445350.
[b.] Department of Organic Chemistry, College of Science, Beijing University of Chemical Technology, Beijing 100029, PR China.
†Electronic Supplementary Information (ESI) available: Details of characterization of the synthesized compounds.. See DOI: 10.1039/x0xx00000x

aromatic substitution (S$_N$Ar) and Suzuki coupling in this study. This synthesis aimed to develop novel cationic cyclopentadienyl iron complexes with long conjugated structures as special optical materials. The complexes are (η^6-1,4-bis((4-methoxyphenyleth-ynyl) phenoxy) benzene) (η^5-cyclopentadienyl) iron hexafluoro-phosphate (**CFS-M**), (η^6-1,4-bis((4-methoxy-phenylethynyl) phenyl)benzene) (η^5-cyclopentadienyl) iron hexafluorophosphate (**CFS-T**) and (η^6-1,4-bis((4-methoxyphenylethynyl) biphenoxyl) benzene) (η^5-cyclopentadienyl) iron hexafluorophosphate (**CFS-D**) (See Chart 1). The methoxy group and cationic cyclopentadienyliron complexes of arenes were selected as the functional donor and acceptor functionalities, respectively. Ethynylphenyl, ethynylene and phenyl spacers were chosen in the design of optical molecules because of their linearity, which allows high planarity and effective conjugation. These spacers also induce strong intra and intermolecular interactions due to their linearity and they generally possess high fluorescence quantum yields with emissions in the blue or violet-blue region.[11] The linear and NLO properties of the prepared complexes were investigated.

Results and discussion

Synthesis

The cyclopentadienyliron complexes of arene were synthesized mainly through S$_N$Ar reaction with various nucleophilic reagents because of the good electron-withdrawing nature of the iron moiety. **CFS-M** and **CFS-D** were prepared through the S$_N$Ar reaction of **Fc-2Cl** with **M-1** and **M-4**, respectively. The synthetic route of the obtained CFSs is shown in Scheme 1. To identify whether the benefit of acetylenic link to extend conjugation, (η^6-1,4-bis(4-methoxyphenoxy)benzene) (η^5-cyclopentadienyl) iron hexafluorophosphate (**CFS-DMo**) was also prepared through the S$_N$Ar reaction of **Fc-2Cl** with 4-methoxyphenol (See Chart 1 and Experimental part).

Recent studies show that cyclopentadienyliron complexes of chloro-substituted arenes can perform efficient Pd-catalyzed cross-coupling reactions with arylboronic acids to form aryl–aryl bonds.[12] **CFS-T** was synthesized via Suzuki coupling reaction to directly generate a C–C bond between the benzene rings of **Fc-2Cl** and **M-3** under mild conditions. The effective catalyst in this coupling reaction is tetrakis(triphenylphosphine) palladium (0). **M-3** was prepared through boric acid ester and **M-2**. The reaction product of boric acid with **M-2** barely showed reactivity in the coupling reaction with **Fc-2Cl**. This result indicates that the methoxy group affected the coupling reactivity of diphenylethynyl chromophores with **Fc-2Cl** to form the C–C bond. The synthesized cationic cyclopentadienyliron complexes were characterized based on their physical data and spectral analysis. The IR spectra of CFSs showed a weak peak at 2215 cm^{-1} to 2220 cm^{-1} that was assigned to the –C≡C– and a strong peak at about 820 cm^{-1} that was assigned to the P–F stretching vibration in PF$_6^-$. The ^{1}H-NMR, ^{13}C-NMR, IR and MS spectra of CFSs were shown in shown in ESI.† All the compounds showed ^{1}H NMR signals for the different kinds of protons at their respective positions. All the data on the compounds confirmed that the structures were correctly synthesized.
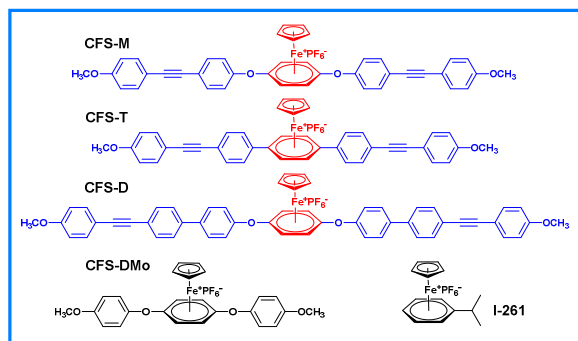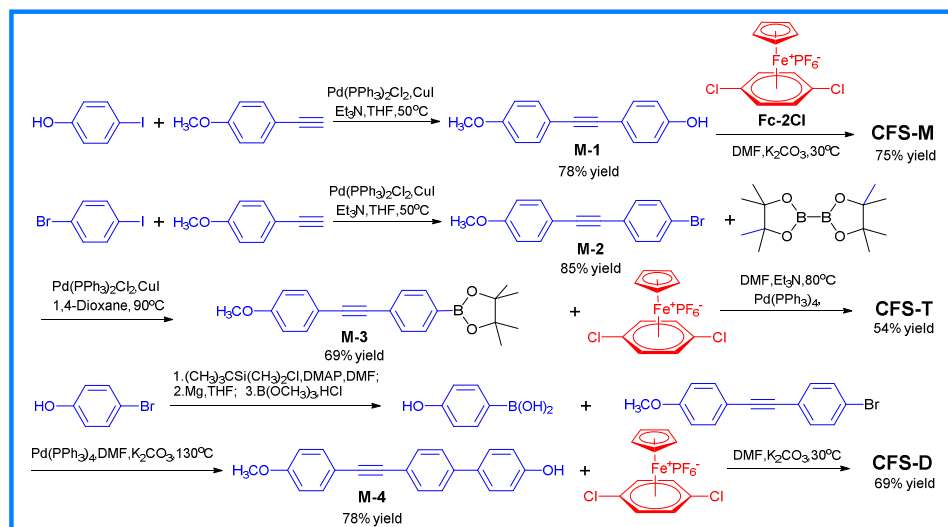

Chart 1. Structure of cyclopentadienyliron complexes of arene studied in this work

Scheme 1. Synthetic route of **CFS-M**, **CFS-T** and **CFS-D** by S$_N$Ar and Suzuki coupling reaction

One-photon spectra

One-photon absorption spectra of **CFS-M**, **CFS-T**, **CFS-D**, **CFS-DMo** and I-261 (Structure is shown in Chart 1) in CH_3CN are shown in Fig. 1, and the corresponding data are presented in Table 1. **CFS-M**, **CFS-T** and **CFS-D** exhibited strong and wide absorptions from 200 nm to 400 nm, while only from 200 nm to 300 nm for **CFS-DMo** which may identify that the introduce of ethynylene spacer in the design of optical molecules can benefit the extension of conjugation. Increasing the conjugation by substituting the phenylacetylene spacer resulted in a red shift in the absorption bands and a stronger absorption in CFSs than in I-261 (λ_{abs} =236 nm, ε=1.02×10^4 M^{-1}cm^{-1}) and **CFS-DMo** (λ_{abs} =226 nm, ε=2.01×10^4 M^{-1}cm^{-1}). The long wavelength absorption band corresponded to the intramolecular charge transfer (ICT) from the electron-donating methoxy group to the electron-withdrawing ferrocenium moiety along the entire conjugate system of the aryl rings and $-C\equiv C-$.[13] Fig. 1 also shows that the maximal absorption peak of CFSs caused by $\pi-\pi^*$ transition became bathochromic as the degree of π delocalization increased. The order of absorption maxima was **CFS-T** > **CFS-D** > **CFS-M**.
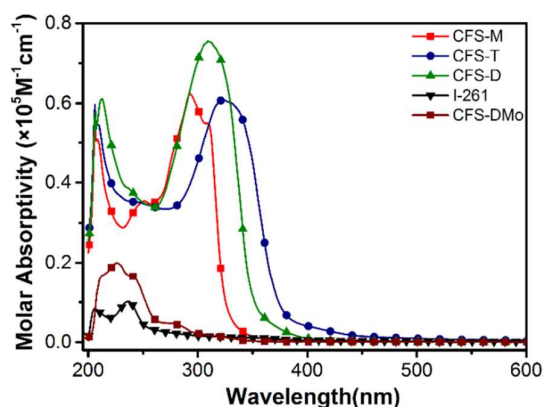

Fig. 1 Quantitative UV-Vis absorption spectra of **CFS-M**, **CFS-T**, **CFS-D**, **CFS-DMo** and I-261 in CH_3CN solution at a concentration of 5×10^{-5} M.

The electron density distribution of the frontier molecular orbital obtained by DFT calculation was analyzed to gain insights into the charge transfer process of the three compounds (Fig. 2). Fig. 2 shows that the HOMOs were mainly localized on the donors and conjugated systems, and the LUMOs were chiefly localized at the cationic cyclopentadienyl iron moieties. This result indicates that the three compounds had good charge transfer abilities in transferring electrons from donor moieties to acceptor moieties.
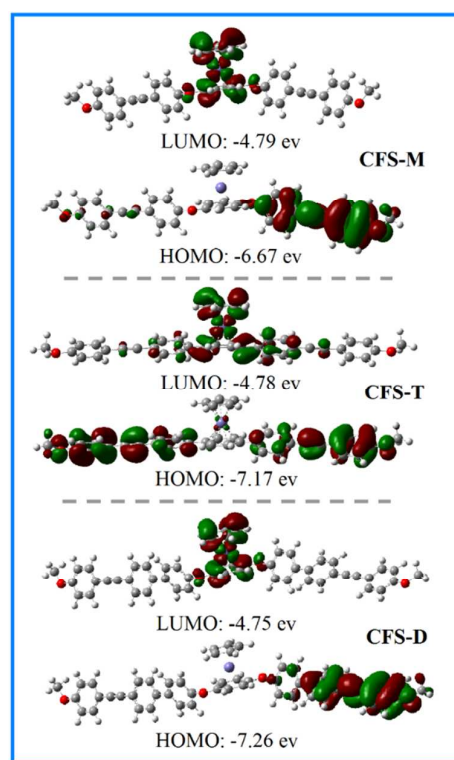

Fig. 2 Electron density distribution of frontier molecular orbitals obtained by DFT calculation of **CFS-M**, **CFS-T** and **CFS-D**.

Table 1. Photophysical parameters as well as DFT calculated data of **CFS-M**, **CFS-T** and **CFS-D**

Compound	λ_{abs}(nm)[a]	ε (M^{-1}cm^{-1})[b]	λ_{em}(nm)[c]	Stokes Shift(cm^{-1})	Φ[d]	HOMO(eV)	LUMO(eV)
CFS-M	294	62400	359	6158	0.45	-6.67	-4.79
CFS-T	325	60800	407	6199	0.72	-7.17	-4.78
CFS-D	311	75600	371	5200	0.64	-7.26	-4.75

[a] Absorption maximum in solution. Concentrations of the CFSs are 5.0 × 10^{-5} M. [b] The molar extinction coefficient at λ_{abs} in solution.
[c] Excited at the absorption maximum. [d] Fluorescence quantum yield, with quinine sulfate as the standard (Φ = 0.54 in 0.1 M H_2SO_4).

Fluorescence emission spectra of **CFS-M**, **CFS-T** and **CFS-D** in the CH_3CN solution are shown in Fig. 3, and the data are also listed in Table 1. These three CFSs all showed fluorescence emission from 350 nm to 500 nm, which was caused by the luminescent processes of the conjugated ligands. Compared with **CFS-DMo**, the maximal emission peaks were red-shifted and the fluorescence intensities increased with the increase in the degree of π delocalization in **CFS-M**, **CFS-T** and **CFS-D**. The maximum emissions of **CFS-T**, **CFS-D**, **CFS-M** and **CFS-DMo** were at about 406, 371, 359 and 333 nm, respectively. The

fluorescence quantum yields of CFSs in CH_3CN solution are also presented in Table 1. From **CFS-M** to **CFS-T**, a gradual increase in conjugation due to the biphenyl and ethynylphenyl spacers led to higher values of the quantum fluorescence yield.
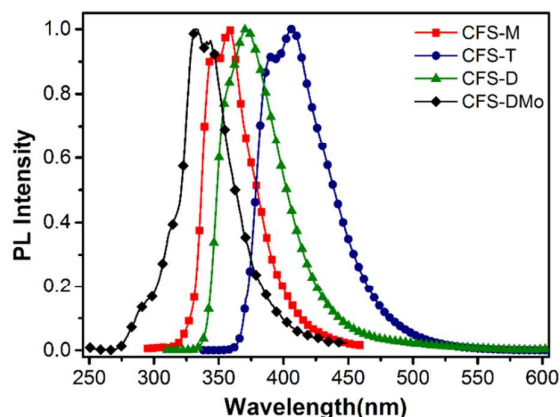

Fig. 3 Normalized emission spectra of **CFS-M**, **CFS-T** and **CFS-D** in CH_3CN solution at a concentration of $5×10^{-5}$ M.

Third-order NLO properties

The nonlinear absorptions of CFSs were measured with nanosecond laser excitation at a visible wavelength of 532 nm, where the compounds showed no linear absorption. Figs. 4 and 5 show the obtained open- and closed-aperture Z-scan curves at an irradiance of 0.15 GW/cm^2. The squares represent the experimental data, and the solid curve is the smoothed line.

Fig. 4 shows that **CFS-M**, **CFS-D**, and **CFS-T** all exhibited an induced positive nonlinear absorption effect, which may be attributed to the D-π-A-π-D structures of CFSs. The cyclopentadienyl iron moiety was the electron acceptor group. The methoxy group was the functional donor, and the triple bonds were located in the conjugated backbone. **CFS-T** and **CFS-D** exhibited higher sufficient capacities in producing a two-photon absorption (TPA) cross section than **CFS-M** due to the extension of the conjugation and the molecular rigidity. **CFS-T** exhibited the strongest electron donating capability because the benzene ring complexing with iron atom and the benzene rings linking −C≡C− of **CFS-T** were via a direct C–C bond, and this nearly planar D-π-A-π-D structure pattern significantly enhanced the NLO properties of these complexes.[14]

Table 2 shows the third-order nonlinear parameters of the complexes. The β values of **CFS-D** and **CFS-T** were 9.43 and 9.61 cm/GW, respectively, which were about 15 times of that of I-261 (0.61 cm/GW). The β value of **CFS-M** was 0.56 cm/GW, which was similar to that of I-261. The values of the TPA cross section (σ) of **CFS-M**, **CFS-D**, and **CFS-T** were $6.89 × 10^{-46}$, $117.03 × 10^{-46}$, and $119.38 × 10^{-46}$ cm^4·s/photon, which were 0.90, 15.3, and 15.6 times of the σ values of I-261 ($7.63 × 10^{-46}$ cm^4·s/photon), respectively.
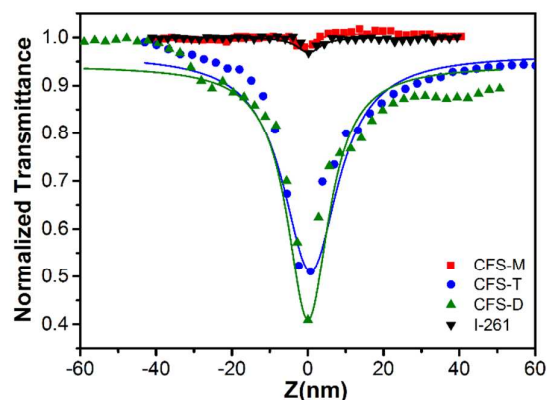

Fig. 4 Normalized transmittance T in open-aperture Z-scan experiments (nanosecond excitation) for **CFS-M**, **CFS-T** and **CFS-D** at irradiance of 0.15 GW/cm^2 in acetonitrile ($5×10^{-4}$ M).
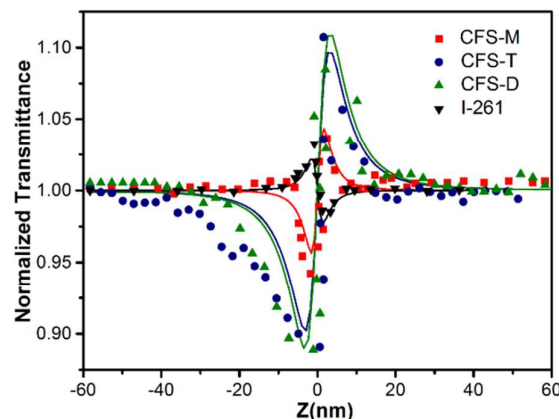

Fig. 5 Normalized transmittance T in closed-aperture Z-scan experiments (nanosecond excitation) for **CFS-M**, **CFS-T** and **CFS-D** with an aperture transmittance of 20% (S=0.2) in acetonitrile ($5×10^{-4}$ M).

Table 2. Z-scan data of **CFS-M**, **CFS-T** and **CFS-D**

Sample^a	γ^b (10^{18}m^2/W)	$n_2{}^c$ (10^{-11}esu)	β^d (cm/GW)	$\chi^{(3)\,e}$ (10^{-12}esu)	σ^f (10^{-46}cm^4·s/photon)
CFS-M	13.91	2.04	0.56	3.35	7
CFS-T	28.76	8.44	9.62	15.78	119
CFS-D	32.45	4.76	9.43	15.92	117
I-261	-7.95	-2.33	0.61	2.06	8

^{a} The samples were prepared as transparent solutions of $5.0×10^{-4}$ M in CH_3CN. ^{b} Optical Kerr constant ^{c} Nonlinear indexe. ^{d} Nonlinear absorption coefficient. ^{e} Third-order optical nonlinear susceptibility. ^{f} nonlinear absorption cross-section.

The closed-aperture Z-scan technique revealed that the four complexes exhibited a nonlinear refractive effect with an aperture transmittance of 20% (S = 0.2) (Fig. 5). The Z-scan set-up was previously calibrated with the standard CS_2 to verify the validity of the measurements. The obtained nonlinear refractive index of CS_2 was 1.36×10^{-11} esu, which was similar to those in previous reports.[15] The values of n_2 obtained from the closed-aperture data were 2.04×10^{-11}, 4.76×10^{-11}, 8.44×10^{-11}, and -2.33×10^{-11} esu for **CFS-M**, **CFS-D**, **CFS-T**, and I-261, respectively. **CFS-M**, **CFS-D**, and **CFS-T** exhibited a valley-peak configuration, corresponding to a positive nonlinear refractive index and a characteristic self-focusing behavior. I-261 exhibited a peak-valley configuration, corresponding to a negative nonlinear refractive index and a characteristic self-defocusing behavior.

Polymerization photoinitiated by CFSs

Cationic polymerization of E51 in the presence of Fc-arenes (1.0 wt%) was carried out under the halogen lamp. In this cationic photopolymerization system, a small amount of epoxy chloropropane was added as the solvent. The results are shown in Fig.6. As shown in Fig.6, these three Fc-arenes all can photoinitiated the polymerization of E51 and the epoxy conversions of photopolymerization system initiated by **CFS-M** can reach 80%, within 400 s of irradiation.
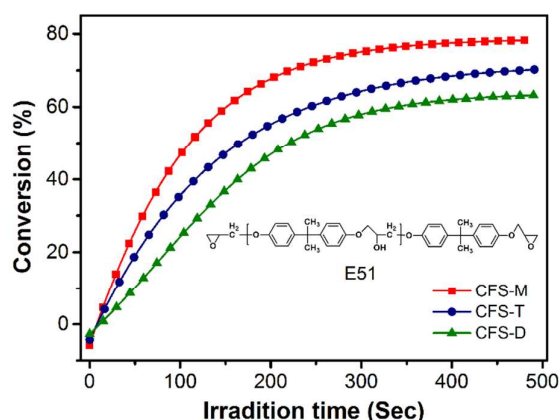

Fig. 6 Photo-polymerization rate of E51 with 3.0 wt. % CFSs.

Conclusions

In this work, three new cationic cyclopentadienyliron complexes with double 4-methoxy diphenylethynyl-substituted arenes were synthesized through Suzuki coupling and S_NAr reactions. The complexes possessed a symmetrical structure, in which a strong acceptor moiety (A), that is, a cationic cyclopentadienyliron moiety, is linked to the donor group (D) via a diphenylethynyl π-bridge. All the molecules exhibited two intense absorptions at 300 nm to 360 nm. With the enlarged and annulated ICT conjugation systems, these compounds exhibited significantly better third-order NLO absorption properties than the commercial cyclopentadienyliron arene complexes I-261. The nonlinear absorption coefficient β of **CFS-T** was about 15 times better than that of I-261, which indicates that the nonlinear absorption properties of cationic cyclopentadienyliron arene complexes can be greatly improved by introducing more diphenylethynyl units to D–A structures. The Z-scan technique revealed that the three complexes exhibited a nonlinear refractive effect. Owing to their polymerization efficiency and large TPA cross-section, these Fc-arenes would have extensive application prospects in the flields of two-photon polymerization.

Experimental

Syntheses

All chemicals used were of analytical reagent grade, which were obtained from commercial sources and used without further purification. (η^6-1,4-Dichlorobenzene) (η^5-cyclopentadienyl) iron hexafluorophosphate (**Fc-2Cl**) and (η^6-cumene) (η^5-cyclopentadienyl) iron hexafluorophosphate (I-261) were prepared through the ligand exchange reaction of ferrocene and arene according to the reference procedure.[16] Starting materials **M-1**[17], **M-2**[18] and **M-3**[19] were prepared according to the extension of reference procedures, and the structures were characterized and confirmed through careful comparison with corresponding literatures. Epoxy resin E51 (from Jiangsu Sanmu Company China) was selected as representative monomer, which is well known in the photopolymerization field and represent excellent structures to evaluate the initiating ability of new systems.

Synthesis of **CFS-DMo**. The compounds **Fc-2Cl** (4.1 g, 10.0 mmol), 4-methoxyphenol (2.5 g, 20.2 mmol) and K_2CO_3 (2.8 g, 20.0 mmol) were stirred in 30 mL of *N, N*-dimethylformamide (DMF) in a 100 mL round bottom flask under a nitrogen atmosphere at room temperature for 8 h. After **Fc-2Cl** was reacted thoroughly, the reaction mixture was transferred into a 15% (v/v) HCl solution, and a granular precipitate was formed. The obtained filtrate was washed by acetone resulting in the dissolution of the product. This solution was then concentrated by evaporating acetone and treated with sufficient KPF_6 in water to allow for the complete precipitation of **CFS-DMo** as a yellow granular solid. The rough product was purified by column chromatography (acetone as eluting agent) and further recrystallized from acetone/ petrol-ether (1:5). Yield=84%. ^{1}H NMR (400 MHz, DMSO-d_6): δ = 7.30 (d, 4H, J = 8.0 Hz), 7.11 (d, 4H, J = 8.0 Hz), 6.17 (s, 4H), 5.20 (s, 5H), 3.82 (s, 6H); ^{13}C NMR (100 MHz, DMSO-d_6): δ = 157.30, 146.23, 130.94, 122.05, 115.60, 77.51, 73.83, 55.54.

Synthesis of **M-4.** A 250 mL of round-bottom flask was charged with (4-hydroxyphenyl) boronic acid (1.10 g, 8.0 mmol), **M-2** (2.01 g, 7.0 mmol), K_2CO_3 (4.40 g, 32.0 mmol),

Pd(PPh$_3$)$_4$ (0.025 g, 0.021 mmol), DMF (50 mL), and water (10 mL). The mixture was heated to reflux and stirred for 8 h. After the reaction, the mixture was poured into a water solution of K$_2$CO$_3$ (200 mL), and then the precipitate was filtered under reduced pressure as a gray solid. The obtained residue was purified by column chromatography on silica gel (petroleum ether as eluting agent) to give the corresponding pure cross-coupling product **M-4** as a white powder.[20] Yield=78%. Mp: 224-226°C. ^{1}H NMR (400MHz, DMSO-d_6): δ = 9.63 (s, 1H), 7.63 (d, 2H, J = 8.3 Hz), 7.54 (d, 4H, J = 8.4 Hz), 7.50 (d, 2H, J = 8.7 Hz), 6.99 (d, 3H, J = 8.7 Hz), 6.86 (d, 2H, J= 8.6 Hz), 3.80 (s, 3H); ^{13}C-NMR (100MHz, DMSO-d_6): δ = 159.48, 157.50, 139.92, 132.87, 131.64, 129.79, 127.71, 125.97, 120.46, 115.81, 114.38, 114.32, 89.81, 88.04, 55.25.

Synthesis of CFS-M. The compounds **Fc-2Cl** (4.1 g, 10.0 mmol), **M-1** (4.5 g, 20.2 mmol) and K$_2$CO$_3$ (2.8 g, 20.0 mmol) were stirred in 30 mL of *N, N*-dimethylformamide (DMF) in a 100 mL round bottom flask under a nitrogen atmosphere at room temperature for 8 h. Reactions were monitored by thin layer chromatography (TLC) using 0.25 mm aluminum-backed silica gel plates. After **Fc-2Cl** was reacted thoroughly, the reaction mixture was transferred into a 15% (v/v) HCl solution, and a granular precipitate was formed. The obtained filtrate was washed by acetone resulting in the dissolution of the product. This solution was then concentrated by evaporating acetone and treated with sufficient KPF$_6$ in water to allow for the complete precipitation of **CFS-M** as a yellow granular solid. The rough product was purified by column chromatography (acetone as eluting agent) and further recrystallized from acetone/ petrol-ether (1:5). Yield=75%. Mp: 214-215°C. ^{1}H NMR (400 MHz, DMSO-d_6): δ = 7.70 (d, 4H, J = 7.5 Hz), 7.52 (d, 4H, J = 8.0 Hz), 7.36 (d, 4H, J = 7.6 Hz), 7.01 (d, 4H, J = 7.9 Hz), 6.39 (s, 4H), 5.27 (s, 5H), 3.81 (s, 6H); ^{13}C NMR (100 MHz, DMSO-d_6): δ = 159.66, 153.53, 133.52, 132.97, 129.57, 120.61, 120.44, 114.43, 113.93, 89.94, 86.95, 78.09, 75.75, 55.28; FT-IR ν(cm^{-1}): 3092.45 (C-H, aromatic), 1588.33, 1536.04, 1471.23 (-C=C-), 832.45(P-F); ESI-MS(m/z): calc. for C$_{41}$H$_{31}$FeO$_4$$^+$ [M]$^+$ 643.1566, found 643.1559 (cation$^+$).

Synthesis of CFS-T. A 100 mL of round-bottom flask was charged with **M-3** (2.0 g, 6.0 mmol), **Fc-2Cl** (1.00 g, 2.4 mmol), Pd(PPh$_3$)$_4$ (5.0 mg, 4.3 µmol), THF (20 mL), and Et$_3$N (50 mL). The mixture was heated to reflux and stirred for 8 h. After the reaction, the mixture was poured into a saturated water solution of KPF$_6$(200 mL), and then the precipitate was filtered under reduced pressure as a brown solid. The obtained residue was purified by column chromatography on aluminum oxide (acetone as eluting agent) to give the corresponding pure cross-coupling product **CFS-T** as a yellow powder. Yield=54%. Mp: 232-234°C. ^{1}H NMR (400 MHz, DMSO-d_6): δ = 8.13 (d, 4H, J = 8.2 Hz), 7.74 (d, 4H, J = 8.2 Hz), 7.57 − 7.56 (m, 4H), 7.11(s, 4H), 7.02 (d, 4H, J = 6.5 Hz), 4.97 (s, 5H) ,3.82(s, 6H); ^{13}C NMR (100 MHz, DMSO-d_6): δ = 159.83, 134.27, 133.12, 131.88 128.25, 124.48, 114.49, 113.80, 101.05, 91.73, 87.42, 85.84, 78.83, 55.32; FT-IR ν(cm^{-1}): 3095.17 (C-H, aromatic), 1528.30, 1502.83, 1457.73 (-C=C-), 828.3 (P-F); ESI-MS(m/z): calc. for C$_{41}$H$_{32}$FeO$_2$$^+$ [M]$^+$ 611.1668, found 611.1662(cation$^+$).

Synthesis of CFS-D. The compounds **Fc-2Cl** (4.1 g, 10.0 mmol), **M-4** (6.1 g, 20.2 mmol) and K$_2$CO$_3$ (2.8g, 20.0 mmol) were stirred in 30 mL of *N, N*-dimethylformamide (DMF) in a 100 mL round bottom flask under a nitrogen atmosphere at room temperature for 12 h. The monitoring method for the reaction and the purification process of the products are similar to the synthesis of **CFS-M**. The final product **CFS-D** was obtained as a yellow granular solid. Yield=79%. Mp: 216-218°C. ^{1}H-NMR (400 MHz, DMSO-d_6): δ = 7.91 (d, 4H, J = 8.2 Hz), 7.79 (d, 4H, J = 7.9 Hz), 7.65 (d, 4H, J = 7.8 Hz), 7.53 (d, 4H, J = 8.3 Hz), 7.45 (d, 4H, J = 8.3 Hz), 7.02 (d, 4H, J = 8.2 Hz), 6.38 (s, 4H), 5.29 (s, 5H), 3.82 (s, 6H); ^{13}C NMR (100 MHz, DMSO-d_6): δ = 159.60, 153.35, 138.60, 137.02, 132.97, 131.83, 129.99, 128.86, 126.85, 121.98, 120.95, 114.42, 114.13, 90.48, 87.7, 77.97, 75.29, 55.28; FT-IR ν(cm^{-1}): 3087.99 (C-H, aromatic), 2214.03 (-C≡C-), 1604.06, 1509.27, 1472.34 (-C=C-), 830.39 (P-F); ESI-MS(m/z): calc. for C$_{53}$H$_{39}$FeO$_4$$^+$ [M]$^+$ 795.2192, found 795.2184 (cation$^+$).

Physical Measurements

The melting points of the compounds were determined using an XT-4 microscopic melting point apparatus. The ^{1}H and ^{13}C NMR spectra were recorded on a Bruker AV400 unity spectrometer. High resolution mass spectra (ESI) were obtained on a Bruker microTOF-QII. FT-IR spectra were recorded on a Nicolet 5700 instrument (Thermo Electron Corporation, Waltham, MA). UV-Vis absorption spectra were recorded on a Hitachi U2500 UV–Vis spectrophotometer (Hitachi High-Technologies Corporation, Tokyo, Japan). An EKSPLA NL303 Q-switched Nd: YAG laser at 532 nm ns laser system was employed to investigate NLO properties of compounds. The fluorescence quantum yields were obtained with quinine sulfate dehydrate (1×10^{-6} mol/L) in 0.1 M sulfuric acid aqueous solution as a reference standard (Φ_{ref} =0.54) by equation (1), [21]

$$\Phi = \frac{A_{ref}\, n^2 F}{A\, n_{ref}^2 F_{ref}} \Phi_{ref}$$

(1)

where Φ is the quantum yield, n is the refractive index, A is the absorbance of solution at the exciting wavelength, and F is the integrated area under the emission spectrum.

The initial geometry optimization was performed with Gaussview (Version 5.0). For all calculation, Gaussian 09 has been employed. The molecular structures in the ground state were optimized based on density function theory (DFT) at the Becke 3-Lee-Yang-Parr (B3LYP)/Genecp (Fe with Lanl2dz basis set and C, H, N, and O with 6-31G** basic set).

Z-Scan measurement

Open-aperture Z-scan measurements were performed to determine the nonlinear transmission of laser light through the samples. The Z-scan gives information about the nonlinear absorption coefficient. The samples were prepared as transparent solutions of 5.0×10^{-4} M in spectroscopic-grade acetonitrile. The samples were placed in 1 mm cuvettes and then irradiated by plane-polarized 5 ns laser pulses at 532 nm from the second harmonic output of a Q-switched Nd:YAG

laser. The laser pulse energy was 6 μJ, and the beam focal spot radius (ω_0) was 16 μm. The laser was run in the single shot mode using a data acquisition program, with an approximate interval of 3 s to 4 s in between each pulse. This low repetition rate prevents sample damage and cumulative thermal effects in the medium.

Assuming a Gaussian temporal profile, we expressed the normalized energy transmittance T(z) as[22]:

$$T(z) = \frac{1}{\sqrt{\pi} q_0(z_0)} \int_{-\infty}^{\infty} \ln\left[1 + q_0(z_0)e^{-t^2}\right] dt \tag{2}$$

where

$$\Delta T_{P-V} = 0.406(1-S)^{0.25}|\Delta\phi_0|$$

$$L_{eff} = [1 - e^{-\alpha_0 L}]/\alpha_0$$

L_{eff} is the effective length of the sample defined in terms of the linear-absorption coefficient α_0; $z_0 = k\omega_0^2/2$ is the Rayleigh length; ω_0 is the beam waist; $k = 2\pi/\lambda$ is the wave vector; λ is the laser wavelength; z is the sample position; I_0 is the on-axis irradiance at the focus (z = 0).

The nonlinear absorption coefficient β can be determined by fitting the Z-scan curves with Eq. (2). The nonlinear absorption cross-section can be determined using $\sigma = h\nu\beta/N$, where hν is the excitation energy and N is the number of molecules per cm^3. Usually, σ is expressed in Goppert–Mayer (GM) units, where $1\,GM = 1\times10^{-50}$ cm^4·s·molecule^{-1}photon^{-1}. The third-order NLO susceptibility $\chi^{(3)}$ values of CFSs were obtained as previously described. [22]

Photopolymerization

Near infrared (NIR) spectroscopy was used to measure the epoxy group conversion as a function of exposure time in the resins. All samples were photocured in 1.8 mm thick plastic molds with a 10 mm diameter center. The molds were clamped between two glass slides. The samples were irradiated with monochromatic light delivered by halogen lamp. The distance is 15cm between irradiation light and sample, the light intensity were 10 mW/cm^{-2}. For each sample, the RT-NIR runs were repeated three times. The specimens were irradiated at different time intervals by manually controlling the curing light. Upon collection of the uncured resin NIR spectrum, spectra were obtained immediately after each exposure interval. The epoxy peak at 6,075 cm^{-1} was used to calculate the epoxy conversion.[23] The epoxy conversion was also calculated by Eq. (3).

$$\text{Conversion \%} = [1 - S_t/S_0] \times 100\% \tag{3}$$

Where S_t is the area of the epoxy C-H characteristic absorbance peak, S_0 is the initial area of the epoxy C-H characteristic absorbance peak.

Acknowledgements

Notes and references

[a]*State Key Laboratory of Chemical Resource Engineering, College of Science, Beijing University of Chemical Technology, Beijing 100029, PR China. E-mail: wangtwj2000@163.com. Tel.: 0086-010-64445350.*
[b]*Department of Organic Chemistry, College of Science, Beijing University of Chemical Technology, Beijing 100029, PR China.*
† Electronic supplementary information (ESI) available: Details of characterization of the synthesized compounds. See DOI: 10.1039/c4ra15424j

1   (a) G. Vives, A. Carella, J.P. Launay and G. Rapenne, *Coord. Chem. Rev.*, 2008, **252**, 1451-1459; (b) A. B. Hadler, V. J. Yannello, W. Bi, E. E. Alp and D. C. Fredrickson, *J. Am. Chem. Soc.*, 2014, **136**, 12073-12084; (c) X.G. Liu and W. Sun, *J. Phys. Chem. A*, 2014, **118**, 10318-10325; (d) P. Paul, M. G. Richmond and S. Bhattacharya, *J. Organomet. Chem.*, 2014, **751**, 760-768.

2   (a) S.J. Wang, Y.F. Wang and C. Cai, *J. Phys. Chem. C*, 2015, **119**, 5589-5595; (b) V. S. V. Satyanarayana, V. Singh, V. Kalyani, C. P. Pradeep, S. Sharma, S. Ghosh and K. E. Gonsalves, *RSC Adv.*, 2014, **4**, 59817-59820; (c) A. Vacher, F. Barrière and D. Lorcy, *Organometallics*, 2013, **32**, 6130-6135; (d) H. V. Nguyen, Z. Zhao, A. Sallustrau, S. L. Horswell, L. Male, A. Mulas and J. H. R. Tucker, *Chem. Commun.*, 2012, **48**, 12165-12167.

3   (a) J. Schmitt, V. Heitz, A. Sour, F. Bolze, H. Ftouni, J.F. Nicoud, L. Flamigni and B. Ventura, *Angew. Chem. Int. Ed.*, 2015, **54**, 169-173; (b) T. Zhao, K. Yu, L. Li, T. Zhang, Z. Guan, N. Gao, P. Yuan, S. Li, S. Q. Yao, Q.H. Xu and G. Q. Xu, *ACS Appl. Mater. Inter.*, 2014, **6**, 2700-2708; (c) H. Zhou, F. Zhou, S. Tang, P. Wu, Y. Chen, Y. Tu, J. Wu and Y. Tian, *Dyes Pigm.*, 2012, **92**, 633-641; (d) J. Lott, C. Ryan, B. Valle, J. R. Johnson, D. A. Schiraldi, J. Shan, K. D. Singer and C. Weder, *Adv. Mater.*, 2011, **23**, 2425-2429; (e) H. M. Kim, B. H. Jeong, J.Y. Hyon, M. J. An, M. S. Seo, J. H. Hong, K. J. Lee, C. H. Kim, T. Joo, S.C. Hong and B. R. Cho, *J. Am. Chem. Soc.*, 2008, **130**, 4246-4247.

4   (a) G. S. He, L.S. Tan, Q. Zheng and P. N. Prasad, *Chem. Rev.*, 2008, **108**, 1245-1330; (b) H. Myung Kim and B. Rae Cho, *Chem. Commun.*, 2009, 153-164.

5   L. Qu, X. Dong, C. Zhong, Z. Liu and J. Qin, *Chem. Phys. Lett.*, 2011, **513**, 103-107.

6   (a) P. Hrobárik, V. Hrobáriková, V. Semak, P. Kasák, E. Rakovský, I. Polyzos, M. Fakis and P. Persephonis, *Org. Lett.*, 2014, **16**, 6358-6361; (b) F. Momicchioli, G. Ponterini and D. Vanossi, *PCCP*, 2014, **16**, 15576-15589; (c) S. Achelle, J.P. Malval, S. Aloïse, A. Barsella, A. Spangenberg, L. Mager, H. Akdas-Kilig, J.L. Fillaut, B. Caro and F. Robin-le Guen, *Chemphyschem*, 2013, **14**, 2725-2736; (d) H. Zhou, Z. Zheng, G. Xu, Z. Yu, X. Yang, L. Cheng, X. Tian, L. Kong, J. Wu and Y. Tian, *Dyes Pigm.*, 2012, **94**, 570-582; (e) P. Hrobárik, V. Hrobáriková, I. Sigmundová, P. Zahradník, M. Fakis, I. Polyzos

and P. Persephonis, *J. Org. Chem.*, 2011, **76**, 8726-8736; (f) V. Hrobáriková, P. Hrobárik, P. Gajdoš, I. Fitilis, M. Fakis, P. Persephonis and P. Zahradník, *J. Org. Chem.*, 2010, **75**, 3053-3068; (g) S. Easwaramoorthi, J.Y. Shin, S. Cho, P. Kim, Y. Inokuma, E. Tsurumaki, A. Osuka and D. Kim, *Chem. Eur. J.*, 2009, **15**, 12005-12017; (h) Z. Liu, T. Chen, B. Liu, Z.L. Huang, T. Huang, S. Li, Y. Xu and J. Qin, *J. Mater. Chem.*, 2007, **17**, 4685-4689.

7   (a) R. L. Roberts, T. Schwich, T. C. Corkery, M. P. Cifuentes, K. A. Green, J. D. Farmer, P. J. Low, T. B. Marder, M. Samoc and M. G. Humphrey, *Adv. Mater.*, 2009, **21**, 2318-2322; (b) L.O. Palsson, R. Pal, B. S. Murray, D. Parker and A. Beeby, *Dalton Trans.*, 2007, 5726-5734; (c) S. Das, A. Nag, D. Goswami and P. K. Bharadwaj, *J. Am. Chem. Soc.*, 2006, **128**, 402-403; (d) Q. Zheng, G. S. He and P. N. Prasad, *J. Mater. Chem.*, 2005, **15**, 579-587.

8   (a) D. J. Roberts, D. Nolan, G. M. O Maille, G. W. Watson, A. Singh, I. Ledoux-Rak and S. M. Draper, *Dalton Trans.*, **2012**, 41, 8850-8860; (c) W. Steffen, M. Laskoski, J.G.M. Morton, U.H.F. Bunz, *J. Organomet. Chem.*, **2004**, 689, 4345-4356; (b) Q.H. Li, R.J. Sa, Y.Q. Wei, K.C. Wu, *J. Phys. Chem. A*, **2008**, 112, 4965-4972.

9   (a) M. Li, Y. Chen, H. Zhang and T. Wang, *Prog. Org. Coat.*, 2010, **68**, 234-239; (b) T. Wang, J. W. Chen, Z. Q. Li and P. Y. Wan, *J. Photochem. Photobiol. A: Chem.*, 2007, **187**, 389-394.

10   (a) J.F. Xing, M.L. Zheng and X.M. Duan, *Chem. Soc. Rev.*, 2015, DOI: 10.1039/C5CS00278H; (b) O. Y. Ciceron, D. A. Carolina, Y. Sheng, L. Gheorghe, V. B. Mykhailo and D. B. Kevin, in *Organic Thin Films for Photonic Applications*, American Chemical Society, 2010, vol. 1039, ch. 8, pp. 111-128; (c) A. Ovsianikov, J. Viertl, B. Chichkov, M. Oubaha, B. MacCraith, I. Sakellari, A. Giakoumaki, D. Gray, M. Vamvakaki, M. Farsari and C. Fotakis, *ACS Nano*, 2008, **2**, 2257-2262.

11   (a) V. Bhalla, G. Singh, M. Kumar, C. Singh, M. Rawat and R. S. Anand, *RSC Adv.*, 2013, **3**, 14722-14730; (b) R. M. Adhikari, L. Duan, L. Hou, Y. Qiu, D. C. Neckers and B. K. Shah, *Chem. Mater.*, 2009, **21**, 4638-4644; (c) R. M. Adhikari, R. Mondal, B. K. Shah and D. C. Neckers, *J. Org. Chem.*, 2007, **72**, 4727-4732.

12   J. Zhao, S. Jin, Y. Weng, Y. Chen and T. Wang, *Ind. Eng. Chem. Res.*, 2014, **53**, 1308-1312.

13   (a) G. L. Li, J. Q. Liu, B. D. Zhao and T. Wang, *Spectrochim. Acta A*, 2013, **104**, 287-291; (b) G. Li, Y. Chen, J. Han, H. Ye, X. Wang and T. Wang, *Dyes Pigm.*, 2012, **94**, 314-319; (c) F. Bureš, O. Pytela, M. Kivala and F. Diederich, *J. Phys. Org. Chem.*, 2011, **24**, 274-281; (d) G.J. Zhao, R.K. Chen, M.T. Sun, J.Y. Liu, G.Y. Li, Y.L. Gao, K.L. Han, X.C. Yang and L. Sun, *Chem. Eur. J.*, 2008, **14**, 6935-6947.

14   W. Zhang and J. S. Moore, *Angew. Chem. Int. Ed.*, 2006, **45**, 4416-4439.

15   (a) B. Yu, G. Yin, C. Zhu and F. Gan, *Opt. Mater.*, 1998, **11**, 17-21; (b) W. Zhao, P.Palffy-Muhoray, *Appl. Phys. Lett.*, 1993, **63**, 1613-1615; (c) H. Toda, C. M. Verber, *Opt. Mater.*, 1992, **17**, 1379-1381.

16   I. U. Khand, P. L. Pauson and W. E. Watts, *J. Chem. Soc. C*, 1968, 2261-2265.

17   R. Chandra, S. Oya, M.P. Kung, C. Hou, L.W. Jin and H. F. Kung, *J. Med. Chem.*, 2007, **50**, 2415-2423.

18   D. Pan, C. Zhang, S. Ding and N. Jiao, *Eur. J. Org. Chem.*, 2011, **2011**, 4751-4755.

19   J. Kulhánek, F. Bureš and M. Ludwig, *Beilstein J. Org. Chem.*, 2009, **5**, 1-5.

20   (a) X.F. Wu, H. Neumann and M. Beller, *Chem. Commun.*, 2011, **47**, 7959-7961; (b) P. D. Ortiz, R. Suardíaz, L. de Vega, G. Hennrich and P. J. Ortiz, *J. Phys. Chem. A*, 2010, **114**, 2939-2944; (c) D. J. Klein, D. A. Modarelli and F. W. Harris, *Macromolecules*, 2001, **34**, 2427-2437.

21   J. Kulhánek, F. Bureš and M. Ludwig, *Beilstein J. Org. Chem.*, 2009, **5**, 101-145.

22   (a) L. Zhang, Z. Shi, L. Zhang, Y. Zhou and S. ul Hassan, *Mater. Lett.*, 2012, **86**, 62-64; (b) M. Sheik-Bahae, A. A. Said, T. H. Wei, D. J. Hagan and E. W. Van Stryland, *IEEE J. Quantum Elect.*, 1990, **26**, 760-769.

23   B. Jiang and Y. D. Huang, *Composites, Part A,* 2008, **39**, 712-717.

Electronic Supplementary Information (ESI) for

Synthesis and Optical Properties of Novel D-π-A-π-D Type Cationic

Cyclopentadienyliron Complexes of Arenes

B. D. Zhao, G. L. Li, Y. Z. Shi, H. Q. Zhang, T. Wang [*]

*Corresponding author. E-mail: wangtwj2000@163.com. Tel.: 0086-010-64445350.

Contents:

Fig. S1 ^{1}H NMR spectrum of **CFS-M** (DMSO-d_6 as the solvent) .

Fig. S2 ^{1}H NMR spectrum of **CFS-T** (DMSO-d_6 as the solvent) .

3
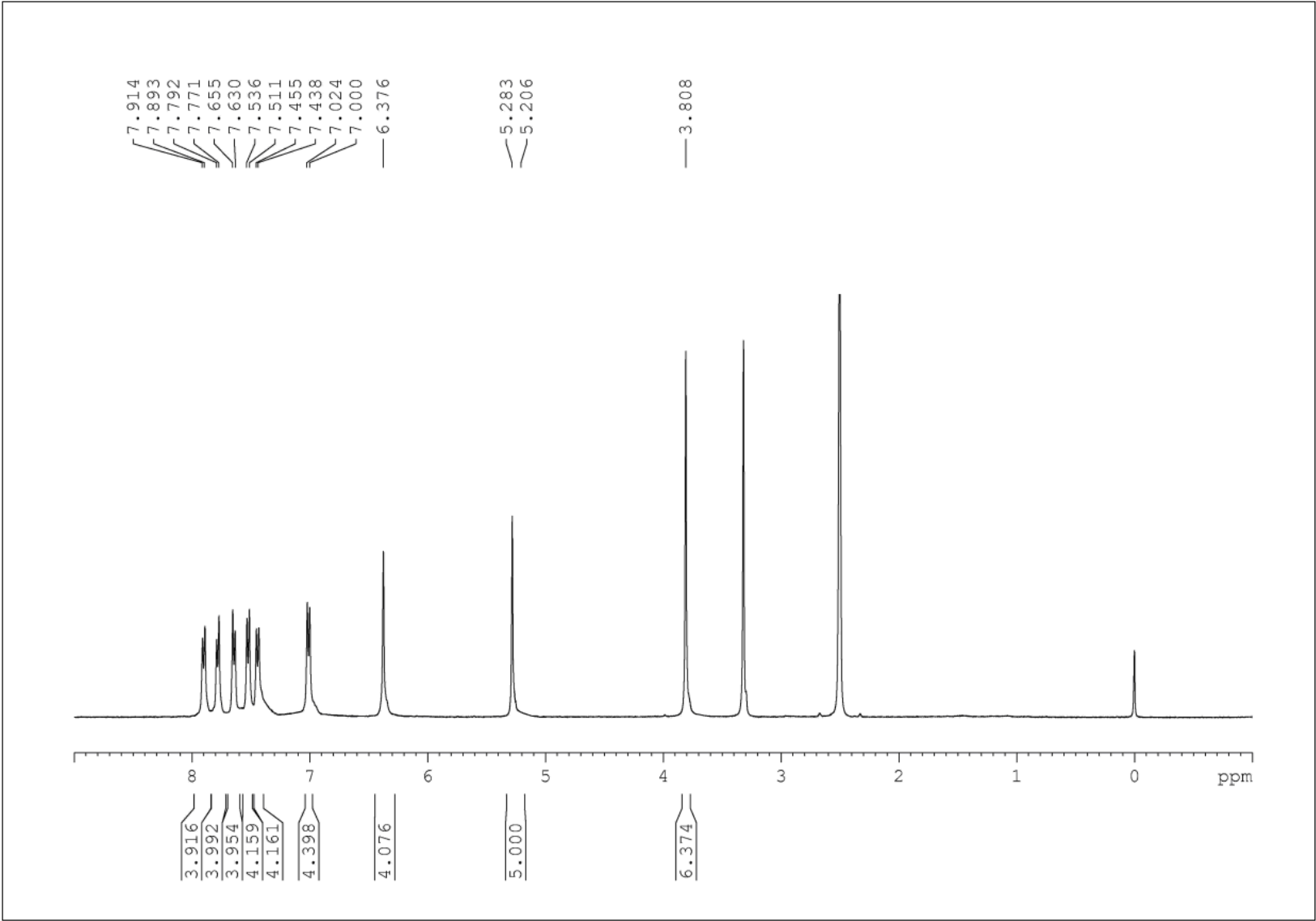
Fig. S3 ^{1}H NMR spectrum of **CFS-D** (DMSO-d_6 as the solvent) .
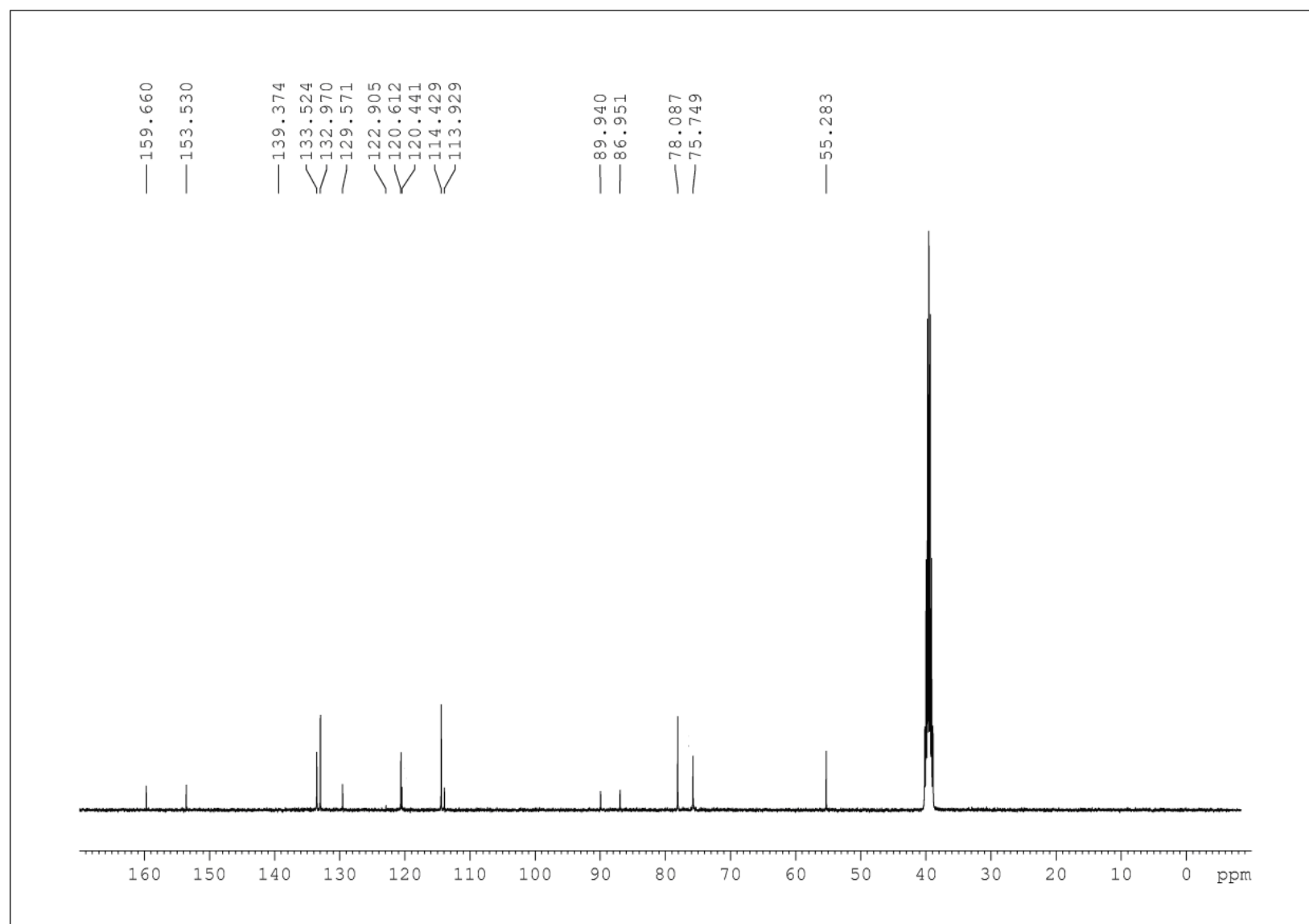
Fig. S4 ^{13}C NMR spectrum of **CFS-M** (DMSO-d_6 as the solvent) .
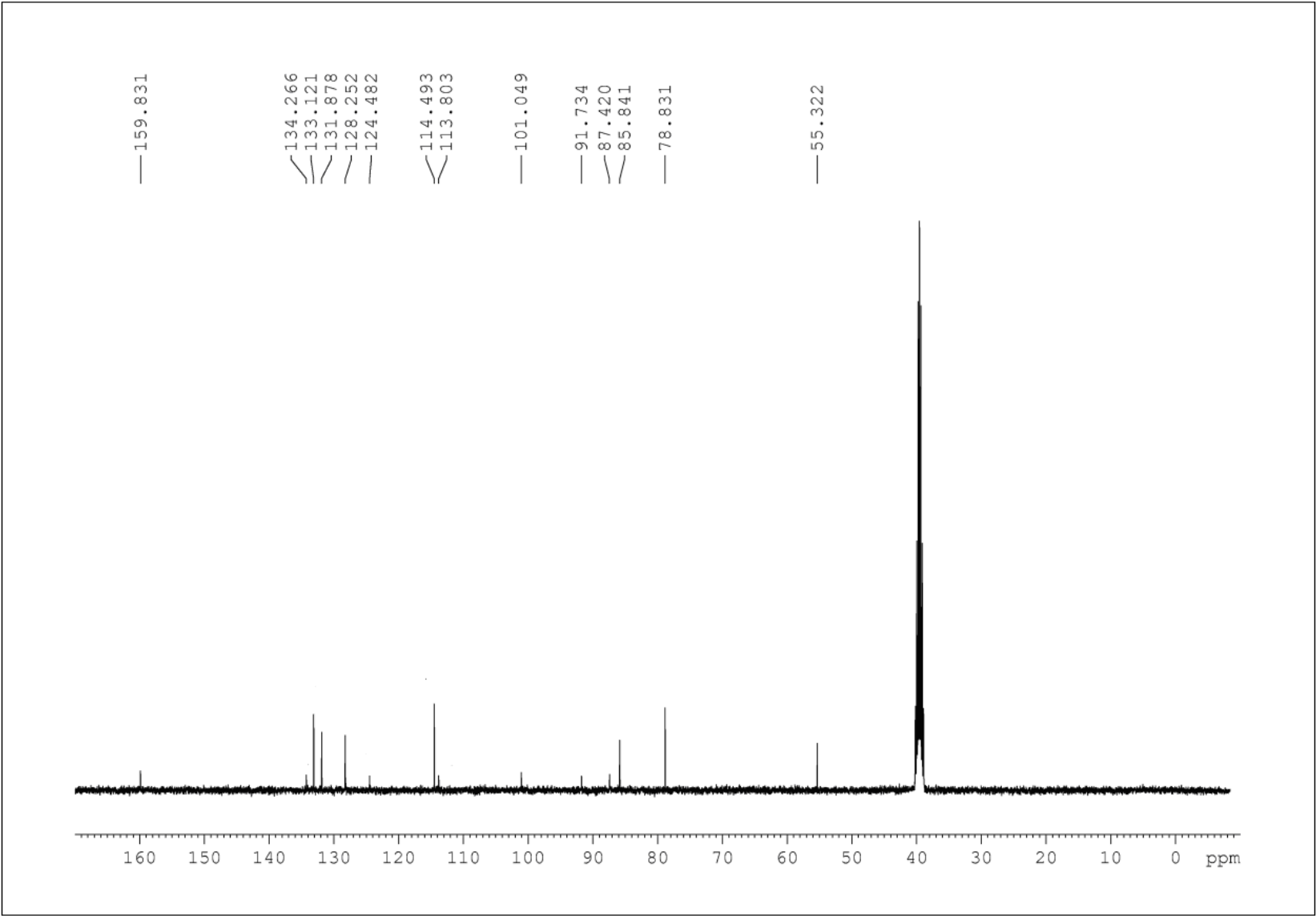
Fig. S5 ^{13}C NMR spectrum of **CFS-T** (DMSO-d_6 as the solvent) .
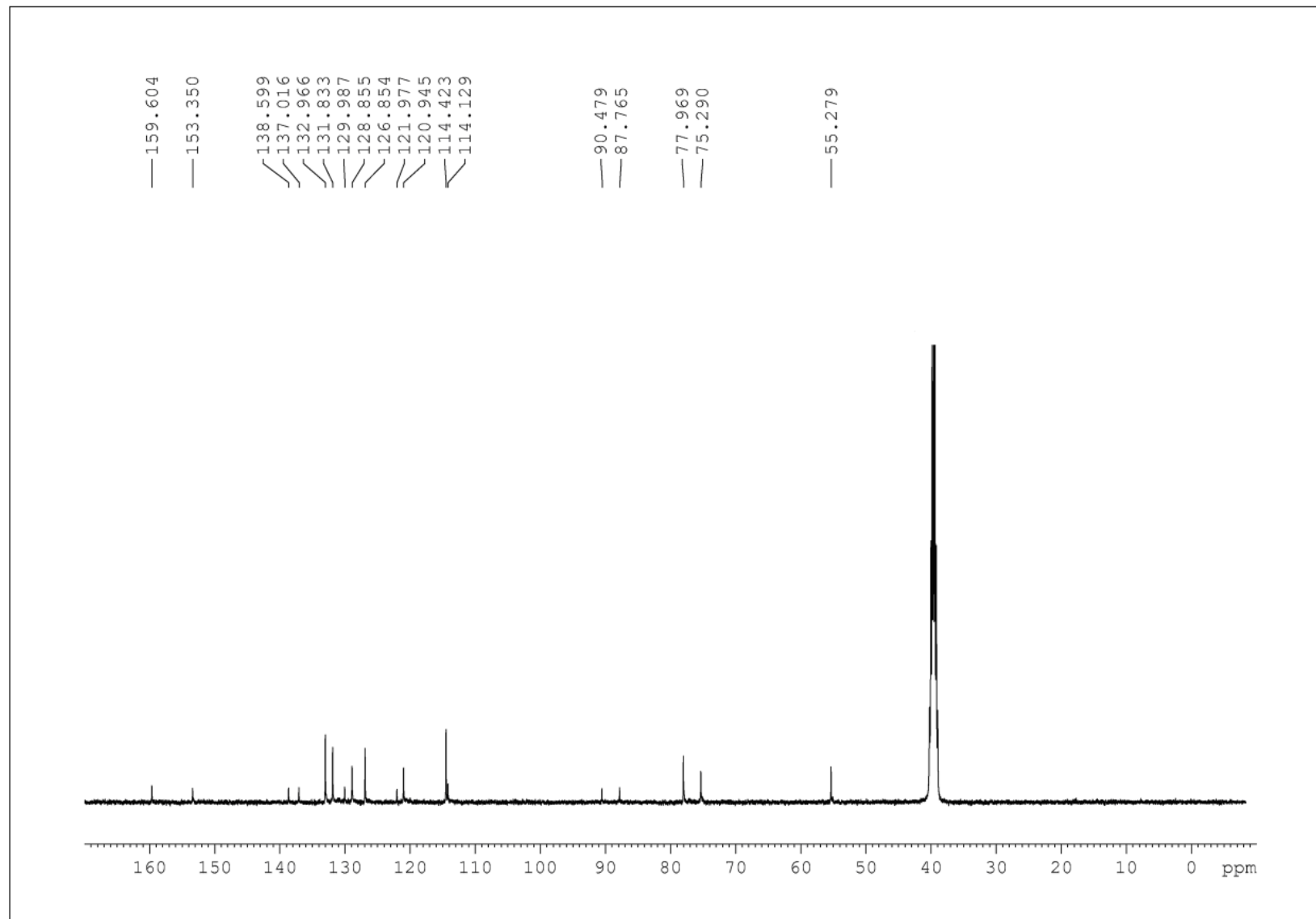
Fig. S6 ^{13}C NMR spectrum of **CFS-D** (DMSO-d_6 as the solvent) .
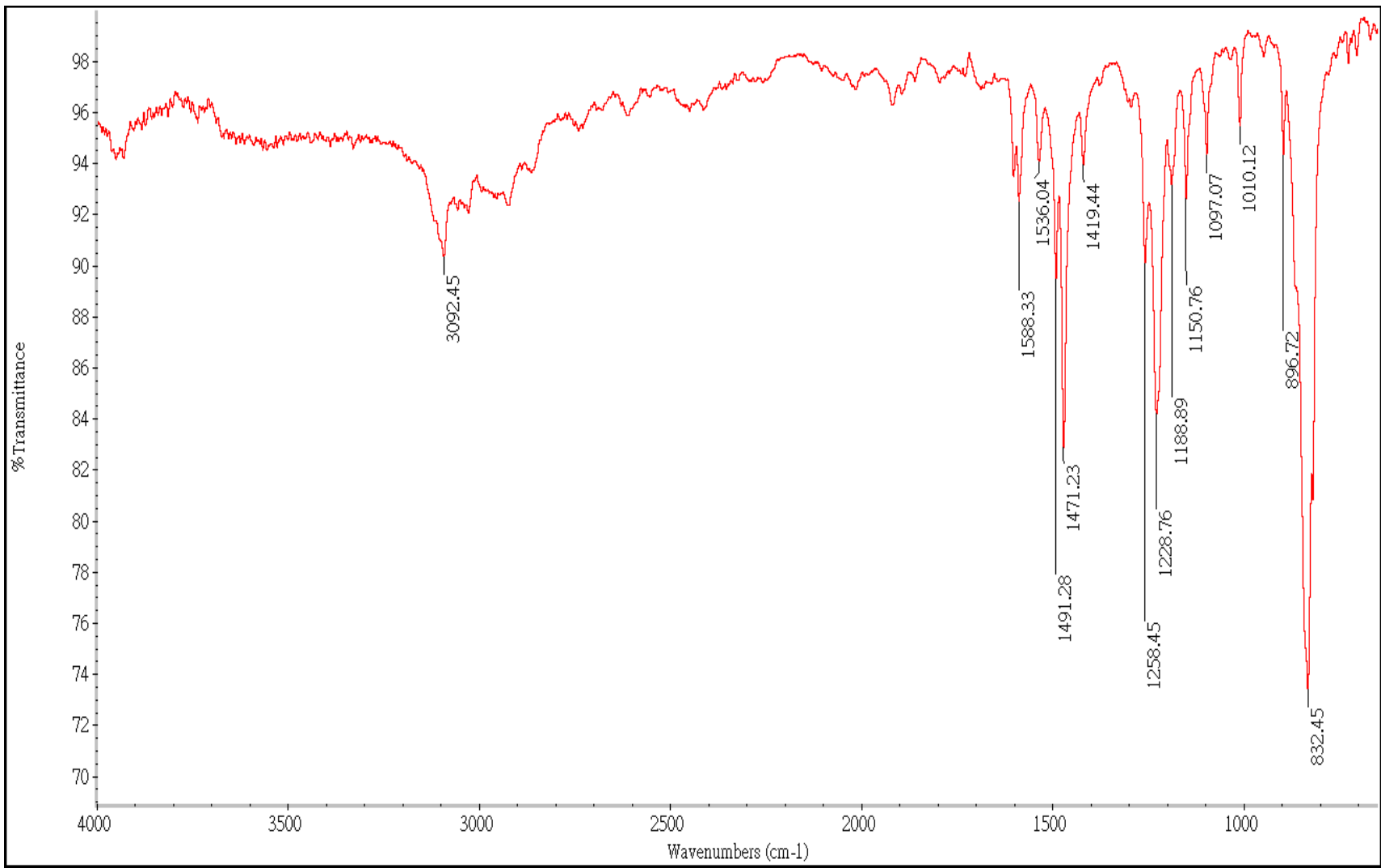
Fig. S7 IR spectrum of **CFS-M**.
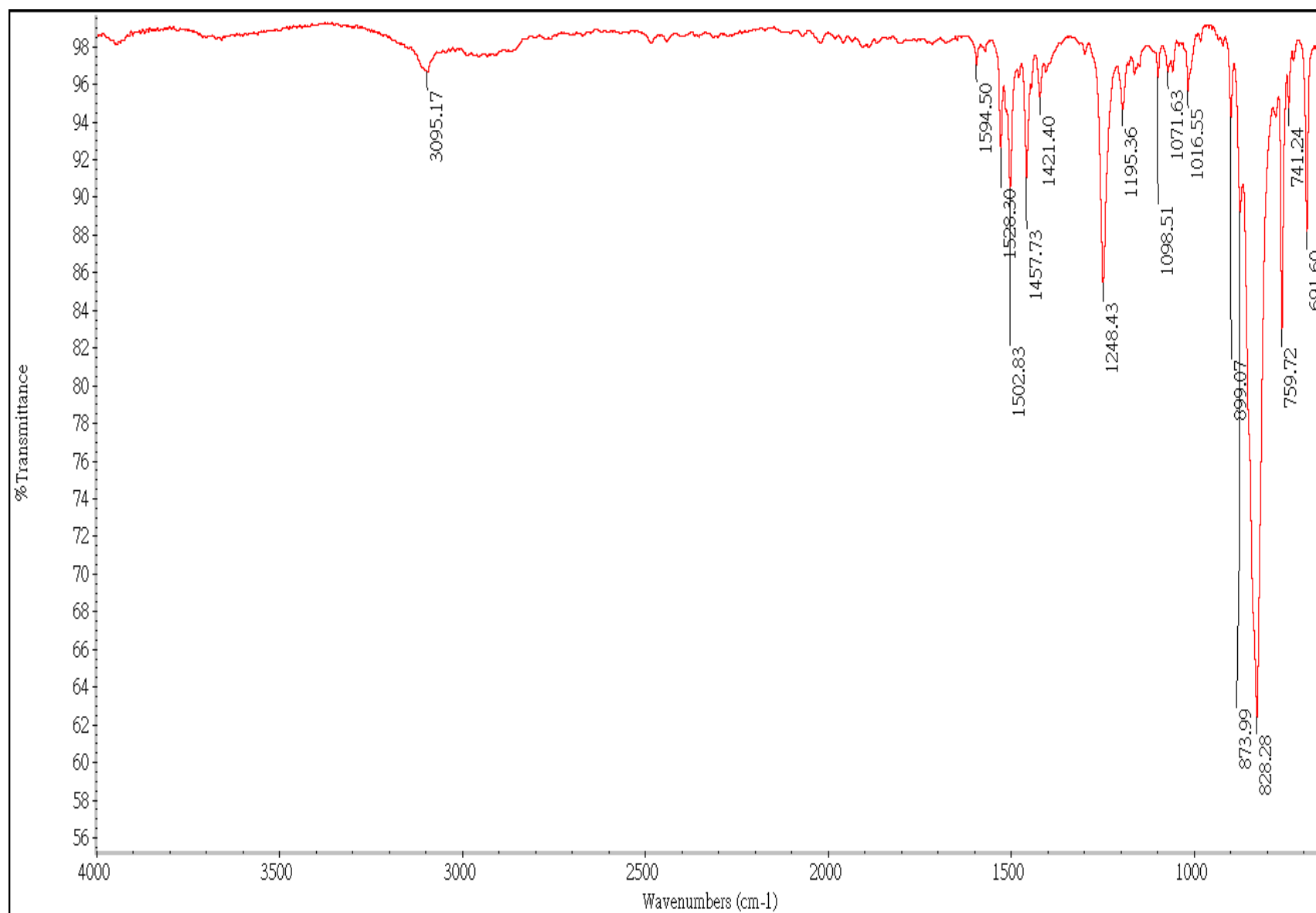
Fig. S8 IR spectrum of **CFS-T**.

9
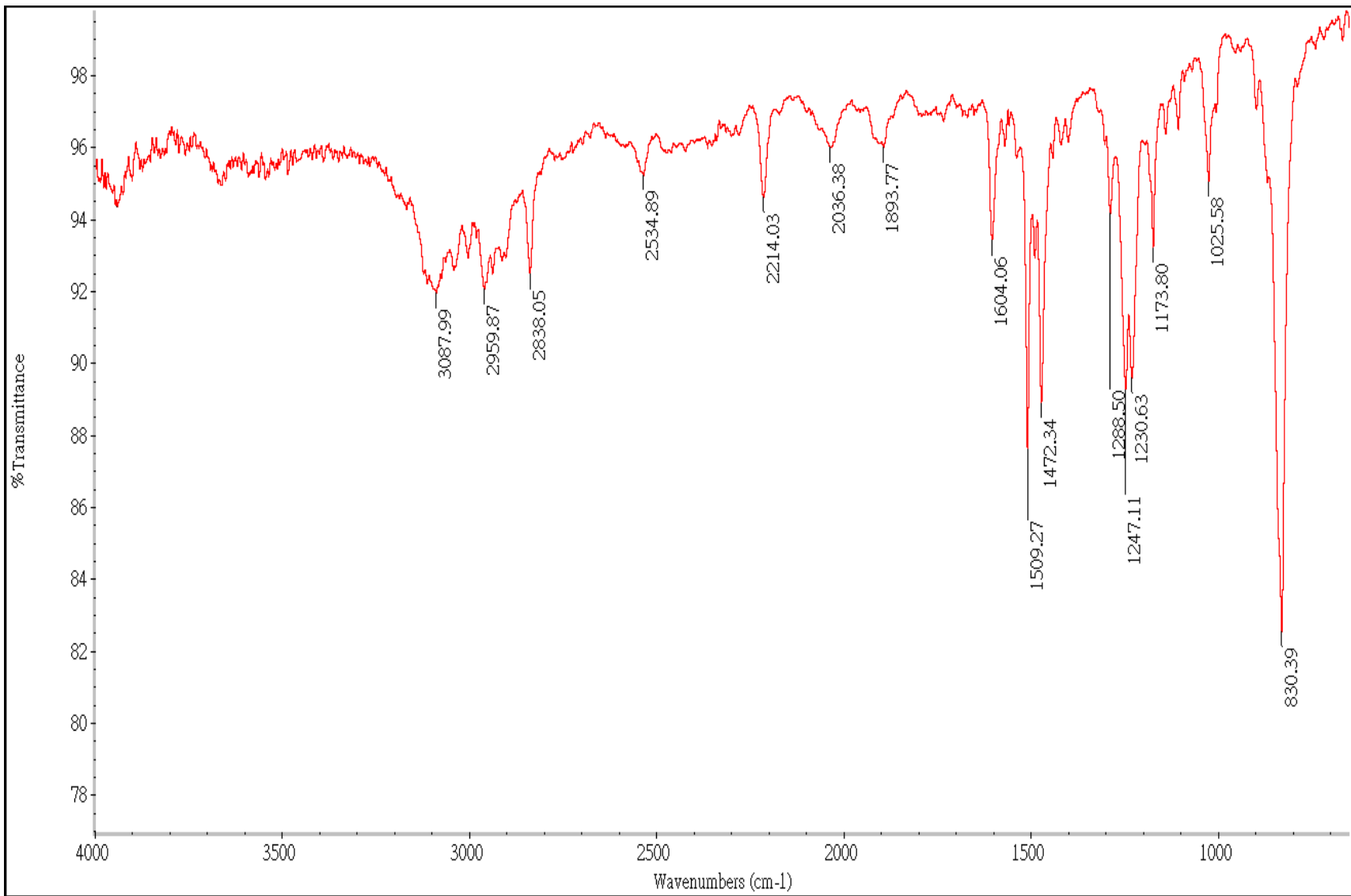
Fig. S9 IR spectrum of **CFS-D**.
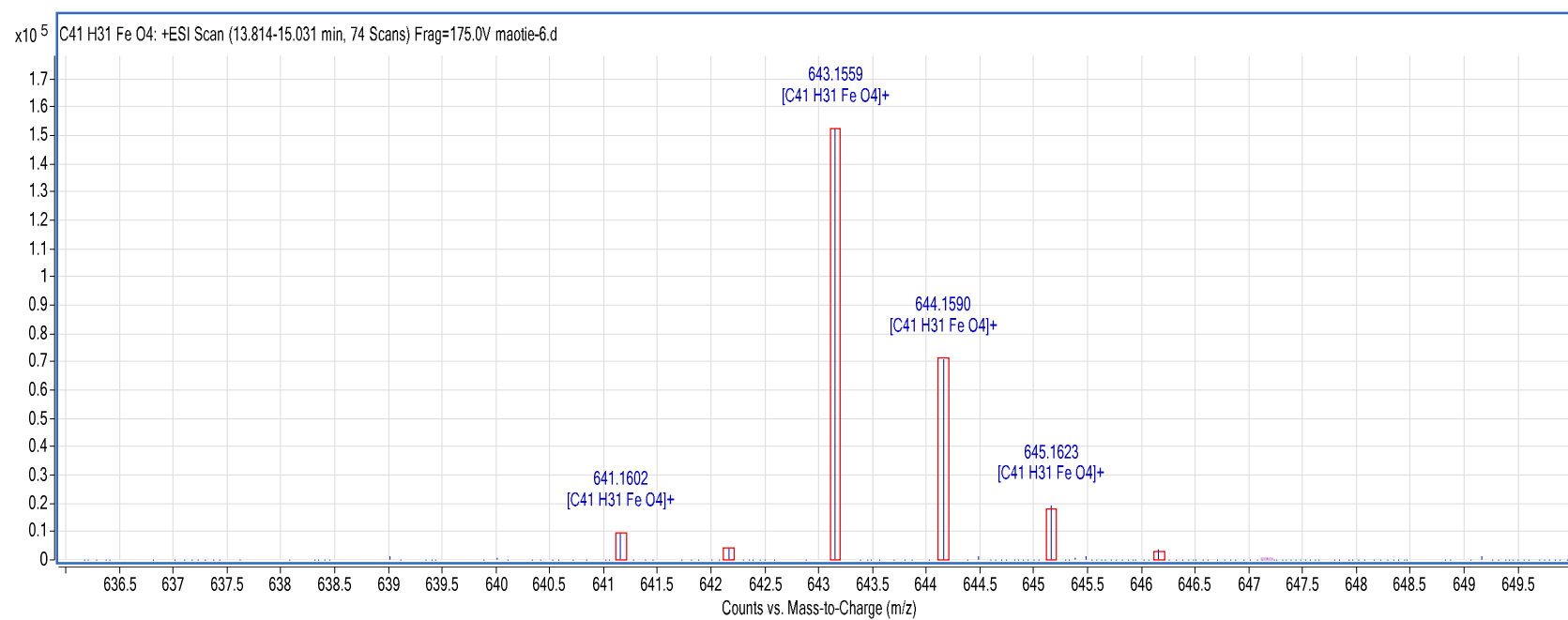
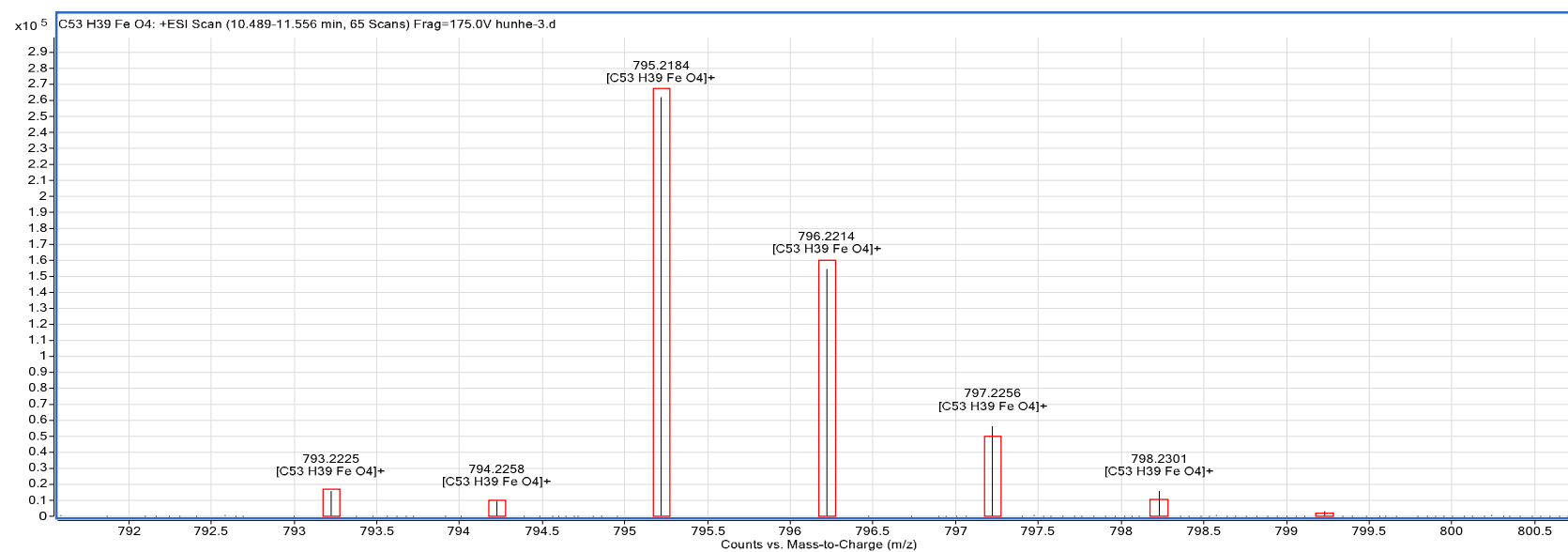**Fig. S10** MS spectrum of **CFS-M**.

11
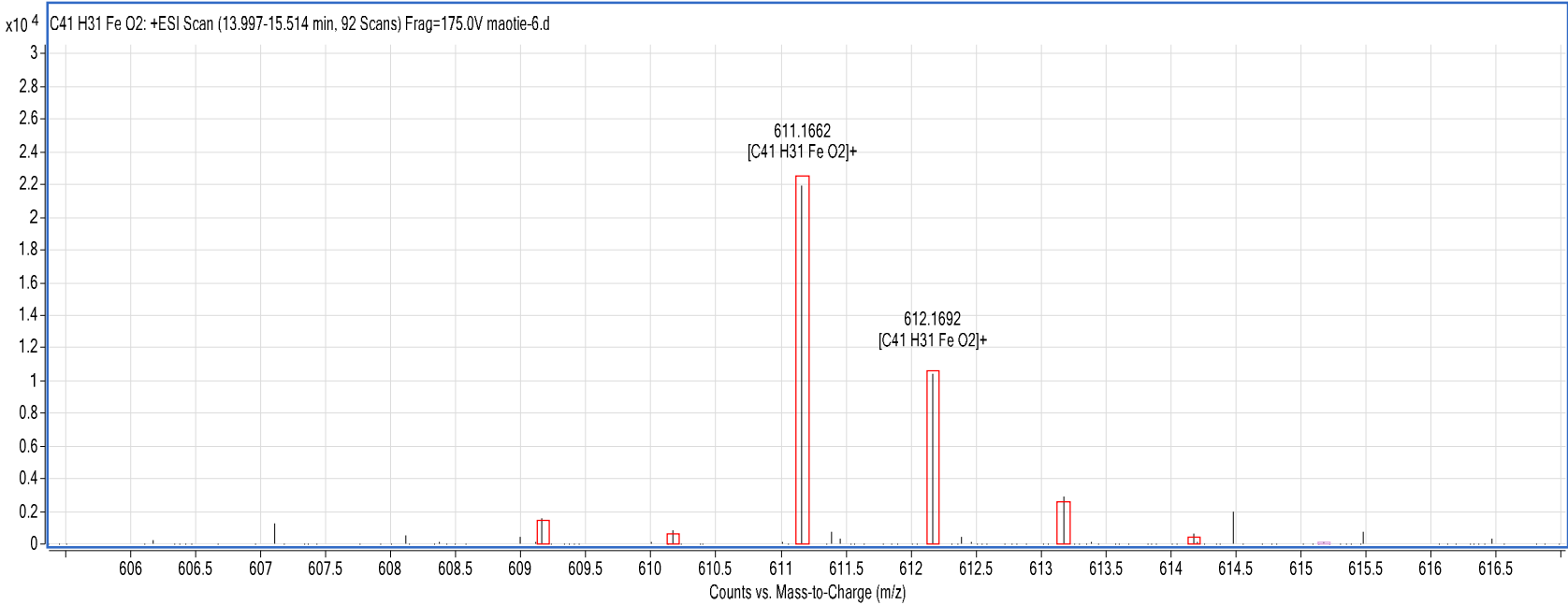
Fig. S11 MS spectrum of **CFS-T**.

Fig. S12 MS spectrum of **CFS-D**.

13